第 49 卷 第 24 期/2022 年 12 月/中国激光 封面文章·研究论文

中国激光

基于多光子聚合微笼阵列的单细胞捕获方法

杨婷[1,2,3]，孙丽娜[1*]，代国朋[1,2,3]，吕孝峰[1,2,3]，王晓朵[2,3**]

[1]东北大学机械工程与自动化学院，辽宁 沈阳 110819；

[2]中国科学院沈阳自动化研究所机器人学国家重点实验室，辽宁 沈阳 110016；

[3]中国科学院机器人与智能制造创新研究院，辽宁 沈阳 110016

摘要 基于飞秒激光单脉冲多光子聚合原理加工出了高纵宽比的微柱阵列，将其与毛细力自组装相结合，有效实现了单细胞阵列的原位限域捕获；通过优化激光加工参数，实现了锥状微柱阵列的高效率加工，并研究了不同激光功率下微柱直径随高度的变化规律；通过优化微柱阵列参数，实现了基于毛细力自组装原理的三维图案化微结构阵列的高通量制备。在此基础上，本团队进行了二氧化硅微球、乳腺癌细胞(MCF-7)单细胞阵列的原位限域捕获实验验证。荧光成像及扫描电子显微镜的表征结果显示，所提方法可以简单、高效地实现单细胞阵列的高通量原位捕获。本研究提供了一种简便、高效的单细胞阵列原位捕获方法，有望应用于生物医学领域单细胞尺寸的相关研究上。

关键词 激光技术；医用光学；光学制造；多光子聚合；毛细力；自组装；单细胞；原位捕获

中图分类号 TN249 **文献标志码** A **DOI**：10.3788/CJL202249.2407104

1 引 言

单细胞分析对于细胞异质学[1-2]、遗传代谢、基因工程及毒性检测等方面的研究具有重要意义[3-4]，而单细胞分析的前提是捕获单个细胞并形成单细胞阵列。目前，常用的细胞捕获方法大多数需要与微流控技术相结合，比如单光束激光法[5-6]、介电泳[7-9]、声镊[10-11]及磁镊[12-14]。介电泳捕获细胞的原理是将细胞在非均匀电场中极化，从而使其在介电泳力的作用下运动或者被势阱限制。声镊则是利用超声驻波产生声压，实现对单细胞的操纵和捕获。显然，利用上述方法捕获细胞时，需要外加电场、磁场等来维持细胞被捕获的状态，一旦取消外加物理场的作用，细胞很容易回到无序状态，不利于后续进一步的表征和分析。因此，发展一种类似于微结构的方式来实现捕获后细胞的固定、培养和观测，是单细胞分析亟待解决的难题。

飞秒激光加工技术具有真三维、非线性吸收和高分辨率等特点[15-17]，不仅可以制备超疏水表面[18]、浸润性表面[19-20]、高精密微孔[21-22]，还可以灵活地在各种透明聚合材料中制造具有超高分辨率的复杂微结构[23-25]。因此，利用飞秒激光加工技术实现对单细胞的原位捕获是一种重要方法。Parmeggiani 研究小组[26]利用激光直写技术加工出了一种能够捕捉微粒的微手，它可以通过光学照明远程控制来抓取小颗粒，但是由于操作方式复杂，难以实现高通量捕获。许兵[27]利用飞秒激光双光子光刻技术，通过在单个目标颗粒周围加工一圈微柱的方式来捕获颗粒，实现了对特定单目标颗粒的捕获；但这种方法需要将捕获目标混入到光刻胶中，不适合用于单细胞的高通量捕获。所查资料显示，目前缺少一种既可以高效率制备微结构，又可以实现细胞高通量快速捕获的方法。

本文发展了一种基于微柱阵列自组装的单细胞捕获方法，实现了人乳腺癌细胞(MCF-7 细胞)的原位捕获。这种方法基于飞秒激光单脉冲多光子聚合原理并结合毛细力自组装有效实现了单细胞的限域被动捕获。本团队首先研究了加工参数对微柱阵列的影响，然后优化微柱的高度和间距，实现微结构与 MCF-7 细胞尺寸的匹配，最后通过细胞原位捕获实验得到了 4×4 的 MCF-7 单细胞阵列。对本文所提方法进行进一步优化，可有效产生大规模的单细胞阵列。本文方法在单细胞水平特异性分析和药物筛选等领域具有巨大的应用潜力。

2 微结构阵列的高通量制备

2.1 单脉冲多光子聚合制备微柱

飞秒激光多光子聚合加工系统主要由飞秒激光光路系统、*X*-*Y*-*Z* 三维精密运动平台、CCD 成像模块和

收稿日期：2022-02-10；**修回日期**：2022-03-22；**录用日期**：2022-03-29

基金项目：国家自然科学基金(61973298)

通信作者：*Lnsun@mail.neu.edu.cn；**wangxiaoduo@sia.cn

软件控制模块组成。本文所用飞秒激光器的波长为1030 nm，重复频率为200 kHz，脉冲宽度为217 fs。针对多光子聚合轴向加工效率较低的问题，本团队采用前期提出的高纵宽比的聚焦光斑进行微柱的单脉冲多光子聚合加工[28]，实验原理如图1(a)所示。为了减小光刻胶(SZ2080，FORTH，希腊；引发剂IRG 369)对聚焦光斑的影响，将光刻胶样本倒置于样品台上，使入射激光先经过盖玻片再进入光刻胶中。激光光束经50倍物镜(NA=0.65，Nikon，日本)聚焦后，光能量分布在后焦体积范围内并呈椭球状。样品上移时，聚焦光斑逐渐进入光刻胶样本中，引发相应区域的光刻胶发生多光子聚合。因此，可以通过调节椭球形光斑浸没到光刻胶中的高度来实现聚合微结构的高度控制，如图1(a)虚线框中放大图所示。当单个飞秒激光脉冲的聚焦光斑呈狭长的椭球形分布时，就可以通过单脉冲曝光实现高纵宽比微柱的多光子聚合加工。将扫描加工后的样本倒置于显影液(正丙醇和异丙醇以1∶1体积比配制而成)中显影6 min，再放入异丙醇溶液中清洗10 min，即可加工得到微柱阵列。在该方法中，单个微柱的加工时间为单个飞秒激光脉冲宽度，即217 fs，可以极大地提高微柱的轴向加工效率。

基于上述加工原理对单脉冲多光子聚合微柱的加工参数进行研究。在实验中，通过移动纳米位移平台对样品高度进行调节，进而实现对微柱高度的精确控制。利用扫描电子显微镜(SEM)表征微柱的高度和直径。图1(b)、(c)给出了激光功率为0.4 W时，单脉冲多光子聚合加工得到的高度分别为5 μm±0.06 μm和40 μm±0.10 μm的微柱阵列，微柱间距分别为5 μm和30 μm。可以看出，微柱呈上窄下宽的圆锥状结构。为探究不同激光功率下微柱底部直径随其高度的变化规律，对0.4～0.8 W激光功率下加工出的高度为5～40 μm(间隔为5 μm)的微柱直径进行统计，统计结果如图1(d)所示。当激光功率一定时，随着微柱高度由5 μm逐渐增加到40 μm，微柱底部逐渐靠近椭球形聚焦光斑的中心部位，微柱底部直径逐渐增大。同时，从图1(d)中还可以看出，当微柱高度相同时，微柱直径随着激光功率的增大而增大。其原因为：由于飞秒激光多光子聚合的能量阈值效应，当入射激光能量增加时，椭球形聚焦光斑的体积会增大，从而使得聚合微柱的直径增大。从图1(d)中可以看出，在0.4～0.8 W的激光功率下，当微柱高度为5～40 μm时，微柱的直径范围为1.86～7.26 μm。以上结果表明，基

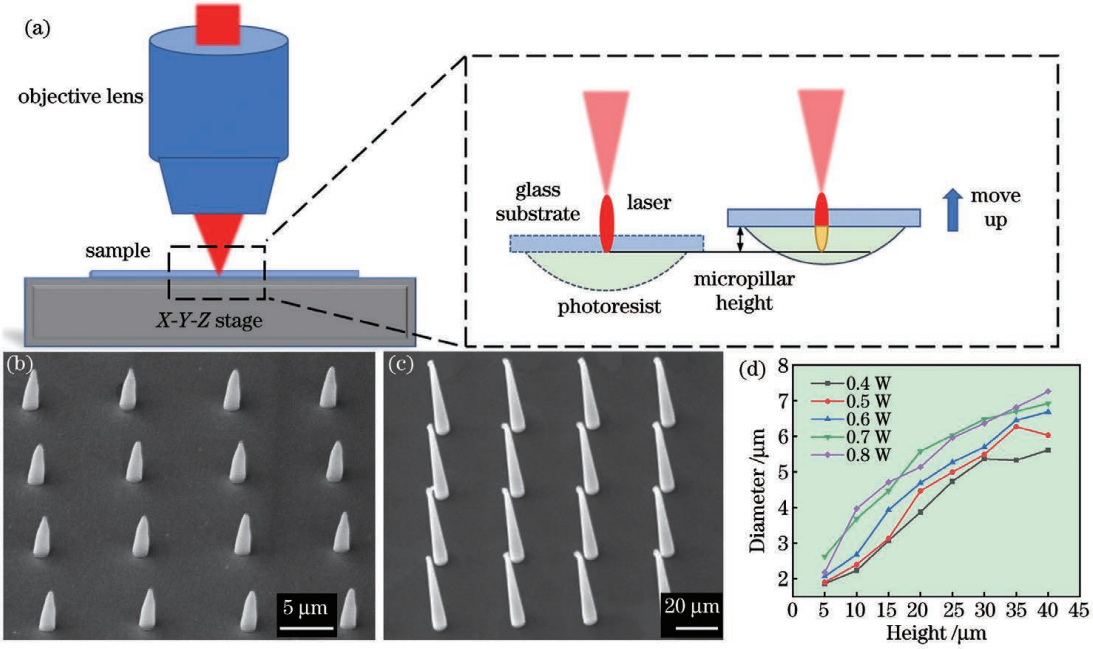

图1　单脉冲多光子聚合实验原理以及加工的微柱阵列。(a)单脉冲多光子聚合原理示意图，右边虚线框内为倒置样品加工过程的细节放大图，红色椭圆形区域代表聚焦光斑的能量分布，黄色区域表示光刻胶中由聚焦光斑引起的多光子聚合区域；(b)(c)单脉冲多光子聚合加工得到的高度为5 μm和40 μm的4×4微柱阵列；(d)入射激光功率为0.4～0.8 W时，微柱直径随高度的变化曲线

Fig. 1　Schematic illustrations of single-femtosecond-laser-pulse-based multiphoton polymerization principle and processed micropillars arrays. (a) Schematic illustrations of single-femtosecond-laser-pulse-based multiphoton polymerization principle, where dotted box on the right shows an enlarged view of the processing of inverted sample, red ellipse area represents energy distribution of laser focal spot, and yellow area represents multiphoton polymerized region caused by the corresponding focal spot in the photoresist; (b)(c) 4×4 micropillar arrays with height of 5 μm and 40 μm processed by single-femtosecond-laser-pulse-based multiphoton polymerization; (d) relationship between micropillar diameter and height when laser power ranges from 0.4 W to 0.8 W

于单脉冲多光子聚合的方法可以实现微柱高度和直径的可控调节，同时该方法可以实现大范围微柱阵列的高效率加工。

2.2　毛细力自组装微结构阵列的制备方法

当微柱之间的距离减小时，随着显影液的挥发，处于液-气界面的两个相邻微柱，其顶端在毛细力作用下有相互靠近的趋势。当相邻微柱间的距离足够近时，微柱受到的静毛细力大于弹性恢复力，微柱间发生毛细力自组装，形成微柱簇结构。值得注意的是，微柱间毛细力的大小既与微柱间距有关，也与微柱高度有关[29]。在微柱间距一定的情况下，微柱受到的弹性恢复力随着微柱高度的增大逐渐减小，当微柱受到的弹性恢复力小于静毛细力时，微柱间同样会发生毛细力自组装。当微柱所受静毛细力与弹性恢复力处于临界状态时，液体挥发过程中发生的不稳定自组装的实验结果如图2(a)所示，其中微柱的间距和高度分别为20 μm和35 μm。可以看出，在临界状态时，微柱阵列的自组装结果较为随机。为实现稳定、可控的毛细力自组装结构阵列的制备，本团队对微柱的间距及高度进行优化。当微柱间距d_1为8 μm、自组装微笼间距d_2为20 μm、微柱高度为25 μm时，微柱可发生稳定的毛细力自组装，如图2(b)所示。图2(b)中的微笼结构由4个微柱自组装而成，从右上角所示的微结构侧视图可以看出，自组装的微柱紧密连接在一起。实验结果显示，将该结构再次浸润于液体环境时，自组装状态仍可继续保持。

鉴于飞秒激光多光子聚合的高空间选择性，将其与本文所提单脉冲微柱多光子聚合方法结合，可以实现多样化三维自组装结构的高通量加工。图2(c)是由8个微柱自组装而成的“四叶草”微笼结构阵列，相邻最近的两个微柱的间距为3 μm，微笼直径d_3为9 μm，微笼间距为21 μm。从图2(c)中可以看出微结构间保持着高度的一致性，证明了该自组装方法的可靠性。此外，通过运动平台路径规划以及激光频率与运动速度的匹配设置，本团队实现了复杂图案化结构的高效率加工。本团队以4个微柱自组装而成的微笼结构为子单元结构进行了复杂三维图案化“SIA”结构的加工，如图2(d)所示，微柱间距为8 μm，自组装微笼间距为15 μm，微柱高度为40 μm，三维尺寸为300 μm×140 μm×40 μm。与图2(b)相比，图2(d)中自组装微笼之间的间距减小，并且自组装后的微笼结构较高。在这种情况下可以观察到自组装的微笼仍可以在毛细力作用下发生二级自组装，出现相邻微笼靠拢的现象。这说明利用二级自组装原理可以实现更加复杂的三维图案化微结构阵列的加工。图2(d)所示“SIA”图案化微结构阵列的多光子聚合时间仅为47 s。与现有单点扫描方法相比，本文所提方法可以极大地提升大范围三维复杂结构的加工效率。

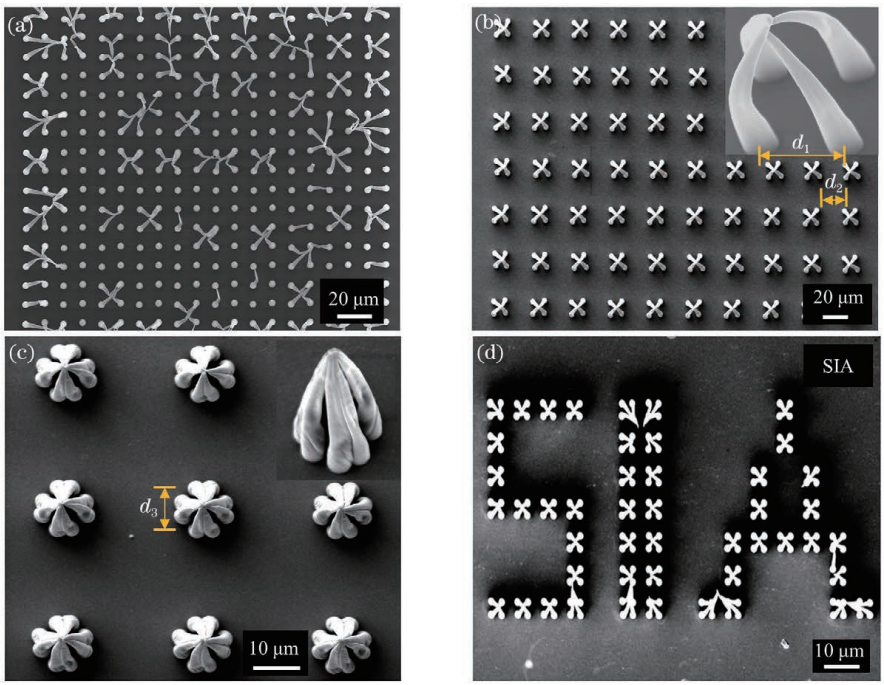

图2　基于毛细力自组装的图案化微结构阵列，其中加工微柱的激光功率均为0.4 W。(a)临界状态时微柱不稳定自组装结果；(b)由4个微柱自组装形成的微笼结构阵列，右上角为单个微笼的侧视放大图；(c)由8个微柱自组装形成的“四叶草”微结构阵列，右上角为侧视放大图；(d)以(b)中自组装结构为子单元加工的“SIA”图案化结构

Fig. 2　Patterned microstructural arrays based on capillary force self-assembly. (a) Unstable self-assembly of micropillars in critical state; (b) microcage arrays assembled by four micropillars, the enlarged view of the microcage structure is shown at upper right corner; (c) “four-leaf clover” microstructure array assembled by eight micropillars, the enlarged view is shown the upper right corner; (d) “SIA” patterned structure consisted by the self-assembled structure in (b) as a subunit

3　单细胞阵列的原位捕获

3.1　微球的原位捕获

在开展基于自组装原理的细胞原位捕获实验之前，首先通过微球原位捕获实验对微柱间隙存在其他物体时微柱的自组装能力进行实验验证。微柱间隙中的物体选取的是直径为10 μm的二氧化硅微球，确保其可在无水乙醇溶液中发生沉降。采用的无水乙醇可在空气中快速挥发，缩短了自组装所需时间。图3(a)是基于毛细力自组装原理的微球捕获过程示意图。具体过程如下：单脉冲多光子聚合的微柱阵列显影完成后，将其从异丙醇溶液中取出，并迅速置于无水乙醇溶液中，在该过程中需保证微柱阵列始终完全浸没于液体环境中；将微球溶液注射到样本微结构所在区域，静置5 min，使微球在重力作用下沉积到样本表面；移除无水乙醇溶液，并用无水乙醇溶液将样本缓慢冲洗2～3次，冲洗掉未落入微结构阵列中的微球；将样本静置于空气中，使其表面残留的溶液自然挥发并进行毛细力自组装，进而实现微球高通量原位捕获。为提高微球的捕获效率，经过参数优化，将微柱的间距设置为12 μm，高度设置为25 μm。图3(b)是无水乙醇溶液中落入微柱之间的微球的光学图像。随着无水乙醇挥发，微柱自组装形成微笼结构，并将落入其中的微球捕获在微笼结构中。图3(c)、(d)分别是被微笼捕获后的微球的光学图像和SEM图像。以上实验结果表明，当微柱间存在直径较小的微粒时，微柱仍可自组装成微笼结构。通过调整微柱的间距和高度，该方法可以实现不同尺寸微球的原位捕获。

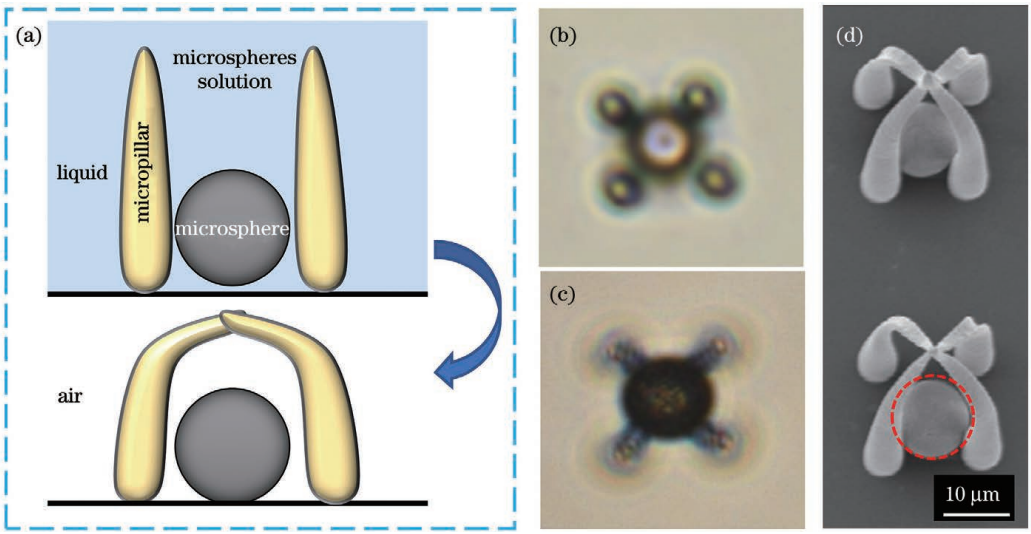

图3　基于毛细力自组装的微球原位捕获。(a)捕获微球的过程示意图；(b)在液体环境中，微球落入微结构的光学图像；(c)在空气环境中，微球被捕获后的光学图像；(d)捕获微球的SEM图，红色虚线圆环中是被捕获的微球

Fig. 3　*In situ* capture of microspheres based on capillary force self-assembly. (a) Diagram of the process of capturing microspheres; (b) optical image of microsphere falling into microstructures in liquid; (c) optical image of captured microspheres in the air; (d) SEM images of microspheres captured, where the captured microsphere is in the red dotted ring

3.2　单细胞阵列的原位高通量捕获

在上述实验的基础上，开展基于毛细力自组装的单细胞阵列的原位捕获实验。与微球相比，MCF-7细胞较为柔软而且不同细胞的形态、尺寸差异较大。考虑到细胞接种过程中的大部分细胞呈球状，更容易落入特定尺寸的微笼中，因此，本团队在微球捕获实验的基础上对实验步骤进行进一步优化，使其适用于柔软、易变形细胞的原位捕获。单细胞阵列原位捕获实验流程如图4所示。首先采用图4(a)、(b)所示的方法加工得到具有不同参数的大范围微柱阵列。然后用磷酸盐平衡生理盐水(PBS)溶液清洗样本，并从样本正上方滴入细胞溶液，使细胞充分落入微结构区域[如图4(c)所示]，细胞密度为120000 cell/mL。接种细胞的样本在细胞培养箱中静置2 h，使细胞充分贴壁并落入微柱间隙底部，如图4(d)所示。接着用含有乙二胺四乙酸(EDTA)的胰酶(胰酶中EDTA的体积分数为0.25%)消化细胞3 min，当约有30%的细胞呈游离状态时，用移液枪轻缓吹打，使细胞脱离微结构。当几乎全部的细胞脱离结构时，加入与胰酶等体积的含10%FBS(胎牛血清)的培养基终止消化，并将脱落的细胞冲洗掉。得益于周围微柱的阻挡，落入微结构内部的细胞被限制在微结构中，如图4(e)所示。然后对样本进行活死染色(Calcein AM · PI)，如图4(f)所示。这样做是为了采用荧光成像方法对细胞的捕获结果进行观测，其中细胞呈绿色，微柱呈红色。最后，移除培养液使其自然挥发，进而使微柱阵列进行毛细力自组装，实现单细胞阵列的原位捕获，如图4(g)所示。

鉴于本文所提方法是一种被动的捕获方式，要求细胞的结构尺寸与微柱自组装形成的微笼结构的尺寸相匹配，因此，首先对消化处理后的MCF-7细胞的直径进行了测量。图5(a)为消化后呈近似球形的MCF-7细胞的光学成像图。对图5(a)中的细胞直径进

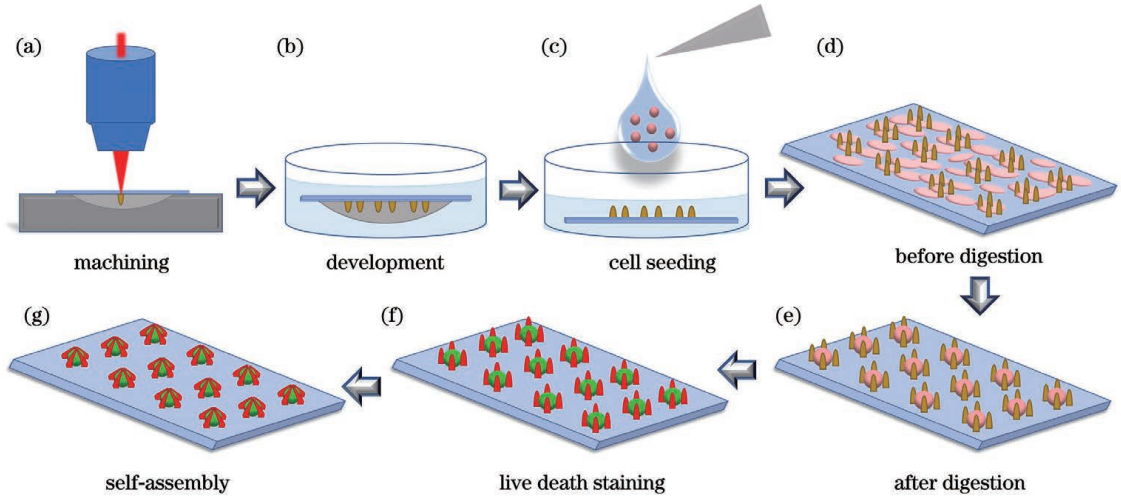

图 4　单细胞阵列原位捕获实验步骤示意图。(a)微结构阵列的扫描加工;(b)微结构倒置显影;(c)细胞接种到微结构样本上;(d)细胞贴壁到样本表面;(e)对样本进行细胞消化处理后得到的单细胞阵列;(f)单细胞阵列活死染色;(g)毛细力自组装实现单细胞阵列的原位捕获

Fig. 4　Schematics of single cell array *in situ* capture experiment procedure. (a) Scanning fabrication of micropillar arrays; (b) inverted development of micropillar structures; (c) cell seeding on microstructural samples; (d) cells adhering to the sample surface; (e) single cell array obtained after cell digestion process; (f) single cell array processed by living dead staining; (g) *in situ* capture of single cell array by capillary-force-based self-assembly of micropillars

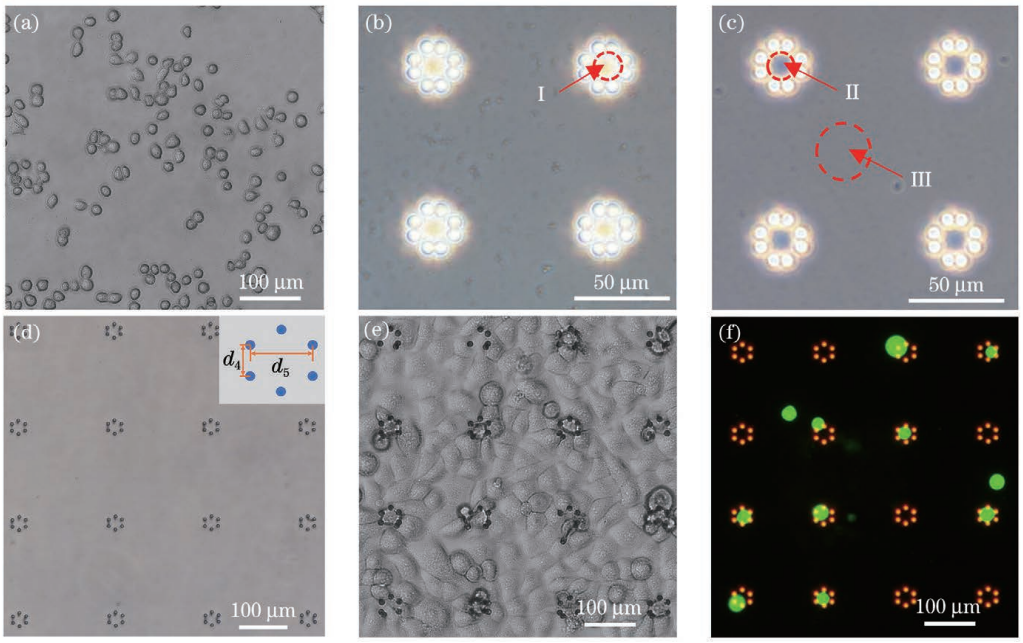

图 5　微笼阵列的单细胞捕获。(a)MCF-7 细胞;(b)(c)除气操作处理前后微结构阵列的光学图像;(d)未接种细胞前,培养液中六微柱微笼阵列的光学图像;(e)接种细胞后,样本表面结构和细胞相对分布的光学图像;(f)消化处理后得到的细胞荧光图像

Fig. 5　Single cell capture in microcage arrays. (a) MCF-7 cells; (b)(c) optical images of microstructure array before and after degassing operation processing; (d) optical image of six micropillars microcage array in culture medium before cell seeding; (e) optical image of sample surface structure and relative distribution of cells after cell seeding; (f) fluorescence images of cells obtained after digestion

行统计分析,可知细胞的直径范围为 18.2 μm±2 μm。微结构间隙小于细胞直径会导致细胞无法进入微结构中而难以捕获;反之,相邻微柱间距大于细胞直径则会难以将细胞有效限制在微笼内。因此,本实验中的微结构直径 d_5 大于 20 μm,相邻微柱间距 d_4 小于 16 μm。为避免显影液影响细胞的存活状态,显影后的样本经去离子水反复清洗后再置于培养液中。然而,在液体置换过程中,微结构中易充满气泡,导致后续细胞无法落入微结构内部。因此,在细胞接种前,将样本浸泡于除气后的空气不饱和去离子水[30]中静置并密封 8 h,使结构内的气泡溶解、清除。图 5(b)、(c)为溶液中微结构除气前后的光学成像,区域Ⅰ和Ⅱ为

微结构内部光学成像，区域Ⅲ为基底在液体中的光学成像。区域Ⅰ和区域Ⅲ成像结果的灰度值相差较大，说明图5(b)中的微结构中存在气泡；区域Ⅱ和区域Ⅲ成像结果的灰度值较为接近，说明经过除气操作后，图5(c)中微结构内部的气泡被清除。这一结果表明，本文所提方法可有效去除微结构内部的气泡，为后续单细胞高通量捕获实验提供了保障。

在上述实验的基础上，本团队开展了基于毛细力自组装原理的单细胞阵列原位捕获实验。在如图5(d)所示的由6个微柱组成的微结构阵列上接种MCF-7细胞，细胞密度为120000 cell/mL。静置2 h后，细胞充分贴壁且几乎铺满整个微结构区域，如图5(e)所示。经消化、荧光染色等操作后得到的4×4单细胞阵列如图5(f)所示，未落入微结构的大多数细胞在消化清洗过程中被液体冲走；部分细胞虽然未落入微结构中，但由于细胞与微结构之间具有较强的黏附力，在消化清洗过程中未被冲走，附着在微笼边沿。当微柱高度为35 μm(直径为5 μm)时，将微结构单元的直径d_5设为24 μm，最大微柱间隙d_4设为10 μm时，消化后的球状细胞更容易落入微结构中，同时可以避免样品冲洗过程中细胞从微笼间隙逃逸。由图5(f)可以看出，被捕获的细胞的尺寸与微结构单元的直径相近，且每个微笼结构中的细胞数量均为1个。这说明该方法可以有效实现单细胞阵列的高通量捕获。与本团队在之前的研究中提出的基于光镊的选择性单细胞定向捕获方法[31]相比，本文所提单细胞被动捕获方法的实验系统更加简单而且易操作，更适合用于尺寸均一单细胞阵列的高通量捕获。

为研究不同自组装微结构的单细胞捕获效果，本团队开展了由不同数量微柱组成的微笼的细胞捕获实验。图6(a)～(c)是四微柱微笼实现细胞原位捕获的荧光图像、光学图像和SEM图像。可以看出，由于结构间隙较大，捕获的细胞很容易被观察到，有利于后续单细胞的原位操作和观测。同时，由于这种结构仅可以捕获尺寸与微笼直径相近的细胞，因此该结构捕获的细胞直径较为统一，可为不同直径的细胞分选提供新方法。图6(d)～(f)是六微柱微笼实现的单细胞阵列的捕获结果，可见，这种结构可以实现不同尺寸细胞的捕获，同时可以通过微柱间隙进行后续的单细胞分析实验。图6(g)～(i)是八微柱微笼捕获的单细胞阵列，可以看出，该结构由于微柱间隔较小，可将捕获的细胞很好地限制在微笼结构中，有望应用于单细胞限域生长特性的研究中。

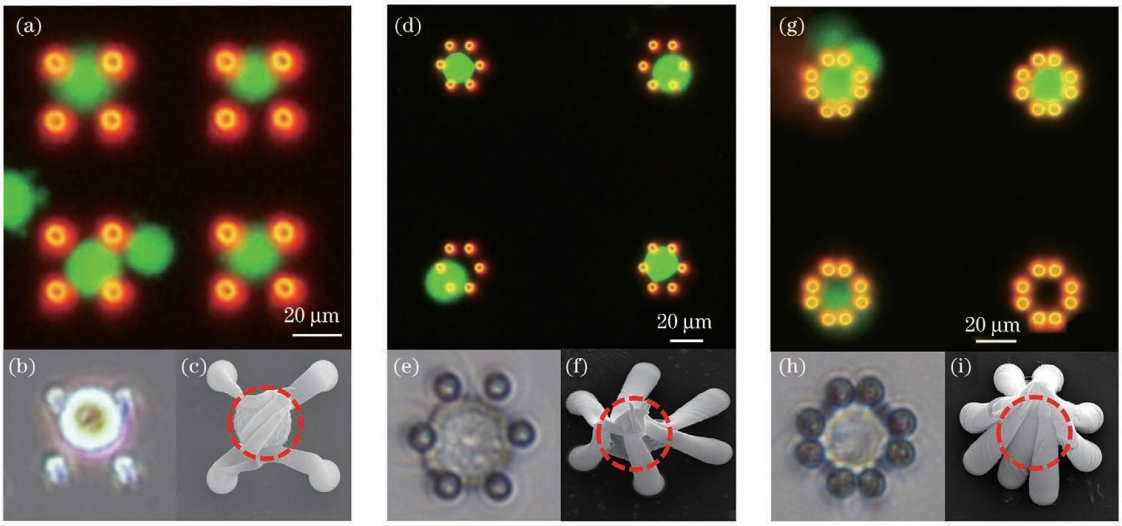

图6　细胞原位捕获图。(a)(b)(c)四微柱结构原位捕获细胞的荧光图像、光学图像及SEM图；(d)(e)(f)六微柱结构原位捕获细胞的荧光图像、光学图像及SEM图；(g)(h)(i)八微柱结构原位捕获细胞的荧光图像、光学图像及SEM图

Fig. 6　Cells *in situ* capture diagram. (a)(b)(c) Fluorescence image, optical image and SEM image of cells *in situ* capture by four micropillars structures; (d)(e)(f) fluorescence image, optical image and SEM image of cells *in situ* capture by six micropillars structures; (g)(h)(i) fluorescence image, optical image and SEM image of cells *in situ* capture by eight micropillars structures

4　结　　论

针对高通量单细胞捕获的应用需求，本团队基于飞秒激光单脉冲多光子聚合技术，结合毛细力自组装原理，提出了一种基于微柱阵列自组装的单细胞阵列限域被动捕获方法，并采用该方法实现了MCF-7单细胞阵列的高通量原位捕获。利用飞秒激光单脉冲多光子聚合实现了高纵宽比微柱阵列的高效制备；通过微柱间距与高度的优化及其大范围路径规划，实现了大范围三维复杂微笼结构的高通量毛细力自组装；通过微笼结构参数与细胞尺寸的匹配，成功实现了基于毛细力自组装的单细胞阵列的原位捕获。所提方法为不同尺寸细胞的分选、捕获及原位观测提供了一种较为简便的方法，有望应用于生物工程、医药分析等领域。

参 考 文 献

[1] He D X, Mao A Q, Zheng C B, et al. Aortic heterogeneity across segments and under high fat/salt/glucose conditions at the single cell level[J]. National Science Review, 2020, 7(5): 881-896.

[2] Galler K, Bräutigam K, Große C, et al. Making a big thing of a small cell: recent advances in single cell analysis[J]. The Analyst, 2014, 139(6): 1237-1273.

[3] Schubert C. Single cell analysis: the deepest differences[J]. Nature, 2011, 480(7375): 133-137.

[4] Weaver W M, Tseng P, Kunze A, et al. Advances in high-throughput single cell microtechnologies[J]. Current Opinion in Biotechnology, 2014, 25: 114-123.

[5] Wang X L, Gou X, Chen S X, et al. Cell manipulation tool with combined microwell array and optical tweezers for cell isolation and deposition[J]. Journal of Micromechanics and Microengineering, 2013, 23(7): 075006.

[6] Ozasa K, Won J, Song S, et al. Autonomous oscillation/separation of cell density artificially induced by optical interlink feedback as designed interaction between two isolated microalgae chips[J]. Scientific Reports, 2016, 6: 24602.

[7] Hunt T P, Westervelt R M. Dielectrophoresis tweezers for single cell manipulation[J]. Biomedical Microdevices, 2006, 8(3): 227-230.

[8] Voldman J, Gray M L, Toner M, et al. A microfabrication-based dynamic array cytometer[J]. Analytical Chemistry, 2002, 74(16): 3984-3990.

[9] Wu C H, Chen R F, Liu Y, et al. A planar dielectrophoresis-based chip for high-throughput cell pairing[J]. Lab on a Chip, 2017, 17(23): 4008-4014.

[10] Petersson F, Nilsson A, Holm C, et al. Separation of lipids from blood utilizing ultrasonic standing waves in microfluidic channels[J]. The Analyst, 2004, 129(10): 938-943.

[11] Guo F, Mao Z M, Chen Y C, et al. Three-dimensional manipulation of single cells using surface acoustic waves[J]. Proceedings of the National Academy of Sciences of the United States of America, 2016, 113(6): 1522-1527.

[12] Zhao L B, Pan L, Zhang K, et al. Generation of Janus alginate hydrogel particles with magnetic anisotropy for cell encapsulation[J]. Lab on a Chip, 2009, 9(20): 2981-2986.

[13] Nisisako T, Torii T, Takahashi T, et al. Synthesis of monodisperse bicolored Janus particles with electrical anisotropy using a microfluidic co-flow system[J]. Advanced Materials, 2006, 18(9): 1152-1156.

[14] Kang J H, Krause S, Tobin H, et al. A combined micromagnetic-microfluidic device for rapid capture and culture of rare circulating tumor cells[J]. Lab on a Chip, 2012, 12(12): 2175-2181.

[15] Begantsova Y E, Zvagelsky R, Baranov E V, et al. Imidazole-containing photoinitiators for fabrication of sub-micron structures by 3D two-photon polymerization[J]. European Polymer Journal, 2021, 145: 110209.

[16] Yang D, Liu L P, Gong Q H, et al. Rapid two-photon polymerization of an arbitrary 3D microstructure with 3D focal field engineering[J]. Macromolecular Rapid Communications, 2019, 40(8): e1900041.

[17] Zheng Y C, Zhao Y Y, Zheng M L, et al. Cucurbit[7]uril-carbazole two-photon photoinitiators for the fabrication of biocompatible three-dimensional hydrogel scaffolds by laser direct writing in aqueous solutions[J]. ACS Applied Materials & Interfaces, 2019, 11(2): 1782-1789.

[18] 白雪, 陈烽. 飞秒激光制备超疏水表面的研究进展[J]. 光学学报, 2021, 41(1): 0114003.
Bai X, Chen F. Recent advances in femtosecond laser-induced superhydrophobic surfaces[J]. Acta Optica Sinica, 2021, 41(1): 0114003.

[19] 吴志鹏, 银恺, 吴俊瑞, 等. 飞秒激光微纳制造水下气体浸润性表面[J]. 激光与光电子学进展, 2020, 57(11): 111418.
Wu Z P, Yin K, Wu J R, et al. Femtosecond laser micro-nano fabrication of underwater gas wettable surface[J]. Laser & Optoelectronics Progress, 2020, 57(11): 111418.

[20] 张明池, 刘子源, 潘宁, 等. 飞秒激光制备不锈钢微纳结构表面的润湿机制研究[J]. 中国激光, 2021, 48(18): 1802001.
Zhang M C, Liu Z Y, Pan N, et al. Wetting mechanism of stainless steel micro-nano structure surface prepared by femtosecond laser[J]. Chinese Journal of Lasers, 2021, 48(18): 1802001.

[21] 郭敏超, 王明娣, 张胜江, 等. FR-4覆铜板飞秒激光微孔加工工艺研究[J]. 中国激光, 2020, 47(12): 1202008.
Guo M C, Wang M D, Zhang S J, et al. Techniques for femtosecond laser processing of micro-holes in FR-4 copper clad laminate[J]. Chinese Journal of Lasers, 2020, 47(12): 1202008.

[22] 王解, 赵宗晨, 江超, 等. 飞秒激光在单模光纤中精密加工微孔及其传感应用[J]. 激光与光电子学进展, 2020, 57(11): 111425.
Wang J, Zhao Z C, Jiang C, et al. Femtosecond laser precision machining of micropores in single-mode fiber and sensing application[J]. Laser & Optoelectronics Progress, 2020, 57(11): 111425.

[23] Zhang S, Li S G, Wan X Y, et al. Ultrafast, high-resolution and large-size three-dimensional structure manufacturing through high-efficiency two-photon polymerization initiators[J]. Additive Manufacturing, 2021, 47: 102358.

[24] Faraji R Z, Prewett P D, Davies G J. High-resolution two-photon polymerization: the most versatile technique for the fabrication of microneedle arrays[J]. Microsystems & Nanoengineering, 2021, 7: 71.

[25] Cardenas-Benitez B, Eschenbaum C, Mager D, et al. Pyrolysis-induced shrinking of three-dimensional structures fabricated by two-photon polymerization: experiment and theoretical model[J]. Microsystems & Nanoengineering, 2019, 5: 38.

[26] Martella D, Nocentini S, Nuzhdin D, et al. Photonic microhand with autonomous action[J]. Advanced Materials, 2017, 29(42): 1704047.

[27] 许兵. 功能化微流控芯片的飞秒激光高效集成技术研究[D]. 合肥: 中国科学技术大学, 2018: 1-112.
Xu B. Research on high efficiency femtosecond laser integration of functional microfluidic chips[D]. Hefei: University of Science and Technology of China, 2018: 1-112.

[28] Wang X D, Yu H B, Yang T, et al. Density regulation and localization of cell clusters by self-assembled femtosecond-laser-fabricated micropillar arrays[J]. ACS Applied Materials & Interfaces, 2021, 13(49): 58261-58269.

[29] Vrancken N, Ghosh T, Anand U, et al. Nanoscale elastocapillary effect induced by thin-liquid-film instability[J]. The Journal of Physical Chemistry Letters, 2020, 11(7): 2751-2758.

[30] 孙玉金. 液滴/气泡与微结构表面的粘附机制研究[D]. 徐州: 中国矿业大学, 2018: 109-111.
Sun Y J. Study of adhesion mechanism between water droplet/bubbles and patterned surfaces[D]. Xuzhou: China University of Mining and Technology, 2018: 109-111.

[31] Li P W, Yu H B, Wang X D, et al. Self-assembled microcage fabrication for manipulating and selectively capturing microparticles and cells[J]. Optics Express, 2021, 29(7): 11144-11157.

Single Cell Capture Method Based on Multiphoton Polymerization Microcage Arrays

Yang Ting[1,2,3], Sun Lina[1*], Dai Guopeng[1,2,3], Lü Xiaofeng[1,2,3], Wang Xiaoduo[2,3**]

[1] College of Mechanical Engineering and Automation, Northeastern University, Shenyang 110819, Liaoning, China;

[2] State Key Laboratory of Robotics, Shenyang Institute of Automation, Chinese Academy of Sciences, Shenyang 110016, Liaoning, China;

[3] Institute for Robotics and Intelligent Manufacturing, Chinese Academy of Sciences, Shenyang 110016, Liaoning, China

Abstract

Objective The study of single cell is of great significance in the fields of cell heterogeneity, genetic metabolism, genetic engineering, and toxicity detection. To identify the functional characteristics of individual cells, individual cell capture must first be achieved. However, most trapping methods require a constant force to keep the cell trapped. When the force decreases or disappears, the cells easily revert to a disordered state, which is very harmful to subsequent characterization and analysis. Therefore, a method for capturing individual cells stably without the use of constant external forces is expected to open up a new avenue for single cell research. This paper proposes a method of rapid capture of single cell during the self-assembly process of micropillars based on femtosecond laser multiphoton processing technology and the principle of capillary force self-assembly. It has fast capture, convenient operation, and a broad application range, and has a lot of potential in bioengineering, drug analysis, and other fields.

Methods High aspect ratio micropillars were prepared by single-pulse femtosecond laser multiphoton polymerization. The height and space of the micropillars can be adjusted by moving the micro/nano translation stages vertically and horizontally. The laser-processed sample was developed upside down by a developer for 6 min to remove the photoresist in the unprocessed area. After the sample was developed, it was washed in isopropanol solution for 10 min to remove any residual developer. To prevent the self-assembly of the sample after developing and cleaning, we put it into a PBS solution immediately. The sample was sealed and degassed for 8 h before being disinfected. Drop the cell solution directly above the micropillar arrays with a density of 1.2×10^5 cell/mL. After seeding cells, the sample was placed in the cell incubator for 2 h to allow the cells to fully adhere to the Petri dish and fall into the bottom of the micropillar gap. Subsequently, the uncapped cells were washed off with trypsin, and the sample was processed using living dead staining. Using a pipette gun, remove the liquid and allow the residual solution to evaporate naturally. The cells between the micropillars were captured during the self-assembly process of micropillars.

Results and Discussions The micropillar structure with a high aspect ratio has a large diameter at the bottom and gradually shrinks to the top, showing a conical shape (Fig. 1). The bottom diameter of the micropillar gradually increases as the height and laser power increase. By shortening the distance between micropillars, increasing the distance between self-assembly structures, and reasonably adjusting the height of micropillars, the micropillars close to each other can be self-assembled based on capillary force, to realize the high-efficiency preparation of largescale three-dimensional (3D) complex patterned self-assembly structures (Fig. 2). The experiment of micropillars' self-assembly driven by capillary force to capture microspheres shows that the micropillars can still be self-assembled into microcage structures when there are particles in the micropillar gap (Fig. 3). Based on the above methods, a single cell array capture experiment was carried out. The results of fluorescence imaging and scanning electron microscope (SEM) images show that this method can realize high-throughput *in situ* capture of single cell array simply and efficiently (Fig. 5). Additionally, the cell capture experiment of microcage composed of a different number of micropillars provides a relatively simple method for sorting, capturing, and *in situ* observation of cells of different sizes (Fig. 6). The four micropillar microscage can only capture cell with similar diameter of the microcage, providing a new method for cells sorting. The six micropillar microscage can capture different sizes of cells, and single cell analysis experiment can be carried out by the micropillars' gap. The eight micropillar microscage can strictly restrict the captured cell well in the microcage and is expected to be used in domain-limited growth characteristics research of single cell.

Conclusions To meet the application requirements of high throughput single cell capture, a domain-limited passive capture method of single cell arrays based on self-assembly of a micropillar array is proposed. Based on femtosecond laser single pulse multiphoton polymerization technology and the capillary force self-assembly principle, this method realizes the high-throughput *in situ* capture of the MCF-7 single cell array. Using femtosecond laser single pulse multiphoton polymerization to achieve the high-efficiency preparation of micropillar arrays with a high aspect ratio. By optimizing the

spacing and height of micropillars as well as largescale path planning, high throughput capillary force self-assembly of a largescale 3D complex microcage structure was achieved. The *in situ* capture of a single cell array based on capillary force self-assembly was successfully realized by matching the structural parameters of the microcage with the size of the cells. Different from the traditional single cell capture methods, such as single cell orientation capture method previously proposed by us, this method provides a relatively simple and efficient method for the sorting, capture, and *in situ* observation of cells with different sizes without the need for continuous additional external force. It has various application prospects in the fields of bioengineering, pharmaceutical analysis, and other domains.

Key words laser technique; medical optics; optical manufacturing; multiphoton polymerization; capillary force; self-assembly; single cell; *in situ* capture